CrossMark

RESEARCH PAPER

Enhanced thermoelectric properties of PEDOT/PSS/Te composite films treated with H_2SO_4

Haijun Song · Kefeng Cai · Shirley Shen

Abstract Firstly, tellurium (Te) nanorods with a high Seebeck coefficient have been integrated into a conducting polymer PEDOT/PSS to form PEDOT/PSS/Te composite films. The Seebeck coefficient of the PEDOT/PSS/Te (90 wt.%) composite films is ~191 μV/K, which is about 13 times greater than that of pristine PEDOT/PSS. Then, H_2SO_4 treatment has been used to further tune the thermoelectric properties of the composite films by adjusting the doping level and increasing the carrier concentration. After the acid treatment, the electrical conductivity of the composite films has increased from 0.22 to 1613 S/cm due to the removal of insulating PSS and the structural rearrangement of PEDOT. An optimized power factor of 42.1 μW/mK^2 has been obtained at room temperature for a PEDOT/PSS/Te (80 wt.%) sample, which is about ten times larger than that of the untreated PEDOT/PSS/Te composite film.

H. Song · K. Cai (✉)
Key Laboratory of Advanced Civil Engineering Materials of Ministry of Education; School of Materials Science and Engineering, Tongji University, 4800 Caoan Road, Shanghai 201804, China
e-mail: kfcai@tongji.edu.cn

S. Shen
CSIRO Manufacturing, Normanby Road, Clayton, VIC 3168, Australia

Introduction

Due to their eco-friendly applications in power generation and refrigeration, thermoelectric (TE) materials are attracting increasing attention as emerging green energy materials. The TE performance of a material is evaluated by the material's dimensionless figure of merit, $ZT = S^2\sigma T/\kappa$, where S is the Seebeck coefficient, σ is the electrical conductivity, κ is the thermal conductivity, T is the absolute temperature, and $S^2\sigma$ is the power factor (PF).

Previous studies have mainly focused on inorganic TE materials, such as Bi_2Te_3, because of their high TE efficiencies (Venkatasubramanian et al. 2001; Cao et al. 2008). However, the high cost of the raw materials, potential for heavy metal pollution, energy-intensive processing, and brittleness limit their widely practical applications (He et al. 2013). Compared with inorganic TE materials, conjugated polymers have been studied as alternative TE materials owing to their unique combination of properties that are atypical of inorganic materials, namely, abundant, mechanical flexibility, low cost, facile processability, and environment friendly (He et al. 2013). Furthermore, the intrinsically low thermal conductivities of conducting polymers that typically range from 0.11 to 0.4 W/mK (Han and Alberto 2011) makes them stand out as potential candidates for TE materials (Pal et al. 2013; Pang et al. 2013).

Among numerous conducting polymers, poly(3,4-ethylenedioxythiophene)/poly(styrenesulfonate) (PEDOT/PSS) is one of the most promising candidates for TE materials because of its high electrical conductivity, water solubility, excellent stability, flexibility, and commercial availability (Wang 2009). Generally, two strategies have been used to increase the power factors of PEDOT/PSS. One is to adjust the TE properties of PEDOT/PSS by controlling their doping levels. A high doping level, i.e., a high carrier concentration, results in a high electrical conductivity and a low Seebeck coefficient, and vice versa. For example, by optimization of the doping level, a ZT value up to 0.25 for a tosylate optimum-doped PEDOT film (Bubnova et al. 2011) and about 0.42 for a PSS-doped PEDOT film at room temperature (RT) (Kim et al. 2013) have been reported (note that the ZT value by Kim et al. is somewhat overstated due to the samples measured for electrical properties being different from that for thermal conductivity and the sample for measuring thermal conductivity being supported by a substrate (Weathers et al. 2015)). Another strategy is to prepare PEDOT/PSS/inorganic composites, by taking the advantages of the low thermal conductivity of the polymer and the high PF of the inorganic fillers (Du et al. 2012). Such as the PEDOT/PSS/SWCNTs (35 wt.%) composite showed a PF of 25 μW/mK^2 with a thermal conductivity kept at around 0.4 W/mK (Kim et al. 2009) and the PEDOT/PSS/SnSe composite showed a PF of 386 μW/mK^2 with a low thermal conductivity of about 0.36 W/mK (Ju and Kim 2016) These composites have enhanced the Seebeck coefficient of the PEDOT/PSS without significant suppression of the electrical conductivity. Besides, the organic-inorganic interfaces will scatter phonons to reduce the thermal conductivity to a much lower value than that of inorganic materials (Yu et al. 2011). As a consequence, much progress has been made for the conducting polymer/inorganic TE materials, including tetrakis(dimethylamino)ethylene-treated PEDOT/CNT composite, PEDOT/PSS/Bi$_2$Te$_3$ composite, PEDOT/PSS/graphene composite, polypyrrole/CNT composite (Wang et al. 2015; Du et al. 2014; Xiong et al. 2015; Song et al. 2016), etc.

Te nanorods possess high Seebeck coefficient and are easily synthesized via a solution process. See et al. (2010) prepared an in situ-synthesized PEDOT/PSS/Te-nanorod composite film with a Seebeck coefficient of 163 μV/K, which is nine times greater than that of pristine PEDOT/PSS. Self-assembled Te-nanorod/polyvinylidene fluoride (PVDF) composite film shows a Seebeck coefficient of 288 μV/K (Dun et al. 2015).

Therefore, Te nanorods are an efficient filler to enhance the Seebeck coefficient of the polymer-based composites. While, the special synthesis conditions make it very difficult to extend to other inorganic nanocrystal/conducting polymer composites. Also, the electrical conductivity of the in situ-synthesized PEDOT/PSS/Te-nanorod composite film and the self-assembled Te-nanorod/PVDF composite film is only 19.3 (See et al. 2010) and 5.5 S/cm (Dun et al. 2015), respectively, which is far from satisfactory. Post-treatment is efficient to increase the electrical conductivity through controlling the doping levels (Bubnova et al. 2011; Kim et al. 2013; Wang et al. 2014, 2015). Therefore, in this work, we first chose Te nanorods as an inorganic filler to integrate with PEDOT/PSS to enhance the Seebeck coefficient of the composite, then H$_2$SO$_4$ treatment was used to further tune the TE properties of the composite, finally a much better TE properties were obtained. This approach can also be used to design and adjust the TE properties of other inorganic nanostructures/PEDOT/PSS composites.

Experimental procedures

Materials

PEDOT/PSS aqueous solution (CLEVIOS PH1000) was purchased from H.C. Starck. Methanol and H$_2$SO$_4$ were obtained from Sinopharm Chemical Reagent Co., Ltd. Ascorbic acid and sodium tellurite (Na$_2$TeO$_3$, 97%) were purchased from Aladdin Industrial Corporation. All the materials were used without further purification.

Synthesis of Te nanorods

Te nanorods were prepared by the method described by Xi et al. (2006). In a typical procedure, 56 mmol ascorbic acid and 2 mmol cetyltrimethylammonium bromide (CTAB) were dissolved in 400 mL distilled water with stirring for 30 min to form a clear solution. Then, 2.5 mmol Na$_2$TeO$_3$ was added with vigorous stirring. The obtained suspension was heated to 90 °C and maintained at the temperature for 20 h. Then, the resulting reaction mixture was cooled down to room temperature naturally. The precipitate was centrifuged at 9000 rpm for 15 min after pouring off the supernatant, and the precipitate was washed with distilled water and centrifuged again. The centrifugation process was repeated

for three times, and finally the precipitate was dried under vacuum at 60 °C for 12 h.

Preparation of PEDOT/PSS/Te nomposite films

The Te nanorods with different weight fractions from 0 to 90 wt.% were firstly dispersed in deionized water by ultrasonication for 30 min. Then, 300 μL of PEDOT/PSS aqueous solution was added into the above Te nanorods dispersion, and the resulting mixture was ultrasonically dispersed for about 1 h and stirred for another 1 h. Finally, the mixture was cast onto the precleaned glass substrates and dried at 60 °C to form dense films.

H_2SO_4 treatment of the PEDOT/PSS/Te composite films

For the H_2SO_4 treatment, 200 μL 9 M H_2SO_4 was dropped onto the PEDOT/PSS/Te composite films placed on a 160 °C heating plate for 10 min. The treated films were then washed by distilled water, and consequently by methanol, and finally annealed at 160 °C for another 10 min.

Measurement and characterization

Electrical conductivity was measured using a steady-state four-probe technique with a square wave current (~10 mA in amplitude) using an Ecopia HMS-3000. The Seebeck coefficient was determined by the slope of the linear relationship between the thermal electromotive force and temperature difference (~5–15 K) between two ends on one side of each film. The synthesized Te nanorods and the phase composition of the prepared composite films were analyzed by X-ray diffraction (XRD) using Cu Kα radiation (D/MAX 2550VB3+/PCII). The morphology was analyzed by a field emission scanning electron microscopy (FESEM; FEI Nova NanoSEM 450) and a transmission electron microscopy (HRTEM; JEM-2100F). The surface composition of the films was analyzed by X-ray photoelectron spectroscopy (XPS) with Al Kα radiation (1486.6 eV) using an ESCALAB 250Xi. Carrier concentrations were measured by Hall Effect Measurement (Ecopia HMS-3000). The thicknesses of the films were determined with a Dektak 150 profilometer, and the thickness of the films with 0, 20, 40, 60, 80, 85, and

90 wt.% Te nanorods is 0.65, 0.77, 1.13,1.74, 2.33, 2.78, and 3.57 μm, respectively.

Results and discussion

The XRD peaks shown in Fig. 1 can be indexed to a trigonal phase of tellurium with lattice parameters of a = 4.456 Å and c = 5.918 Å, which are in good agreement with the standard data (JCPDS card no. 36-1452, a = 4.458 Å and c = 5.927 Å). No other phases were detected, indicating that the pure Te nanorods are obtained. The chemical reactions involved in this process are as follows:

$$TeO_3^{2-} + 2H^+ \rightarrow TeO_2 + H_2O \qquad (1)$$

$$C_6H_8O_6 + TeO_2 \rightarrow C_6H_4O_6 + Te + 2H_2O \qquad (2)$$
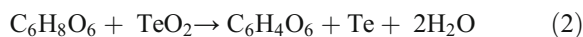
Anionic surfactant CTAB has been widely used in preparing nanowires acting as an excellent soft template (Murphy and Jana 2002). In the present synthetic process, the possible function of CTAB is to generate large number of elongated rodlike micellar structures in an aqueous solution, which may act as soft template for the formation of 1D nanostructures as well as for stabilizing the nanorods. Besides, CTAB also helps to enhance the anisotropy of tellurium and decrease the diameter of the resulting nanowires (Xi et al. 2006).

The morphology of the prepared Te nanorods and PEDOT/PSS/Te composite is characterized by TEM and is shown in Fig. 2. The as-prepared Te nanorods
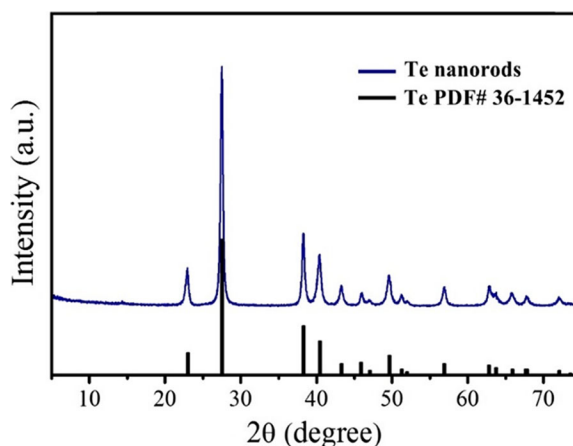
**Fig. 1** XRD pattern of the as-fabricated Te nanorods

have a uniformly distributed size with diameter around 20 nm and length up to 200–300 nm. For the PEDOT/PSS/Te composite, it can be seen clearly that a thin layer of PEDOT/PSS (about 3 nm) is coated on the surface of Te nanorods (Fig. 2b). Similar phenomenon has been observed in a polyaniline/Te composite by Wang et al. (2016). This interfacial adhesion between PEDOT/PSS and Te nanorods arises from the interactions between the van der Waals forces from the Te atom layers and π interactions from the PEDOT/PSS chains. Besides, due to the templating effect of Te nanorods (Fig. 2c), the PEDOT/PSS interfacial layer possesses a higher degree of organization than the bulk PEDOT/PSS, which may promote the carrier transport in the composite.

Figure 3 shows the surface FESEM images of the PEDOT/PSS/Te composite films with different Te contents. The pristine PEDOT/PSS film shows a very smooth surface. For the PEDOT/PSS/Te composite films, when the Te content is low, i.e., 20 wt.%, part of the Te nanorods randomly distribute in the PEDOT/PSS matrix (the bright area in Fig. 3b) and part of the Te nanorods agglomerate into each other to form bundles (Fig. 3b, inset). As the content of Te nanorods in the composite further increases, the bright areas, corresponding to Te nanorods (including Te nanorods bundles), become larger (Fig. 3c, d), resulting in more routes for the transport of carriers, which will be beneficial to both electrical conductivity and Seebeck coefficient of the PEDOT/PSS/Te composites (see the TE properties hereinafter).

The room-temperature TE properties of the PEDOT/PSS/Te composite films are shown in Fig. 4. As the Te nanorods integrated into PEDOT/PSS increases from 0 to 90 wt.%, the Seebeck coefficient monotonically increases from 15.4 μV/K for the pristine PEDOT/PSS to 191 μV/K. The enhancement is mainly caused by the high Seebeck coefficient of the Te nanorods (~370 μV/K, in accordance with the values of reported bulk Te nanowire film with a Seebeck coefficient of 408 ± 69 μV/K (See et al. 2010; Coates et al. 2013)). The value is close to that reported for conducting polymer/Te composites, being 204 μV/K for a PANI/Te composite (Wang et al. 2016) and 202 μV/K for a reduced graphene oxide/PEDOT/PSS/Te composite (Choi et al. 2016). The electrical conductivity of the pristine PEDOT/PSS film is 0.22 S/cm. As the Te nanorods in the composites increases from 0 to 40 wt.%, the electrical conductivity almost keeps a constant, whereas as the Te content further increases, the electrical conductivity increases monotonically and reaches 0.89 S/cm when Te content is 90 wt.%. The calculated PF is 3.25 $\mu W/mK^2$ for the sample containing 90 wt.% Te nanorods. Note that the electrical conductivity of the as-prepared Te nanorods was only 0.05 S/cm. The electrical conductivity usually cannot exceed the greater value of either individual component in a two-phase

Fig. 2 TEM images of **a** the as-prepared Te nanorods, **b** PEDOT/PSS/Te composite, and **c** a schematic illustration of the preparation procedure of PEDOT/PSS/Te composite films
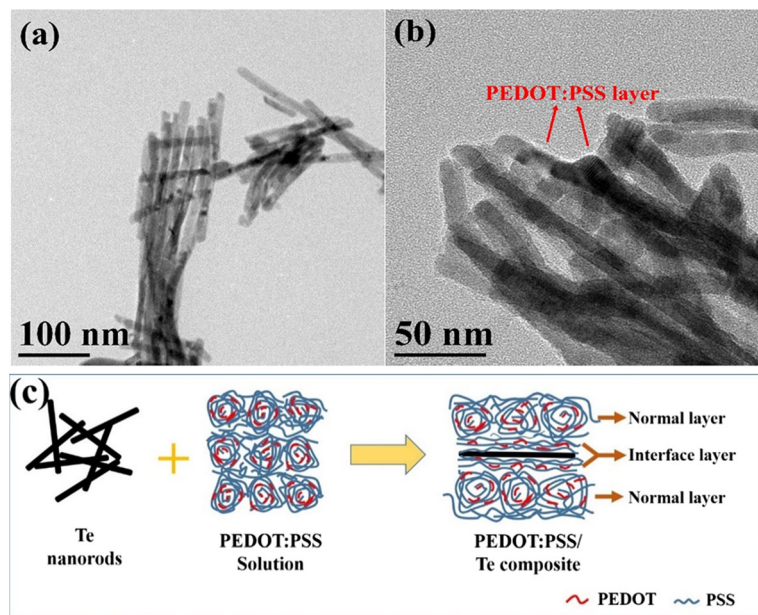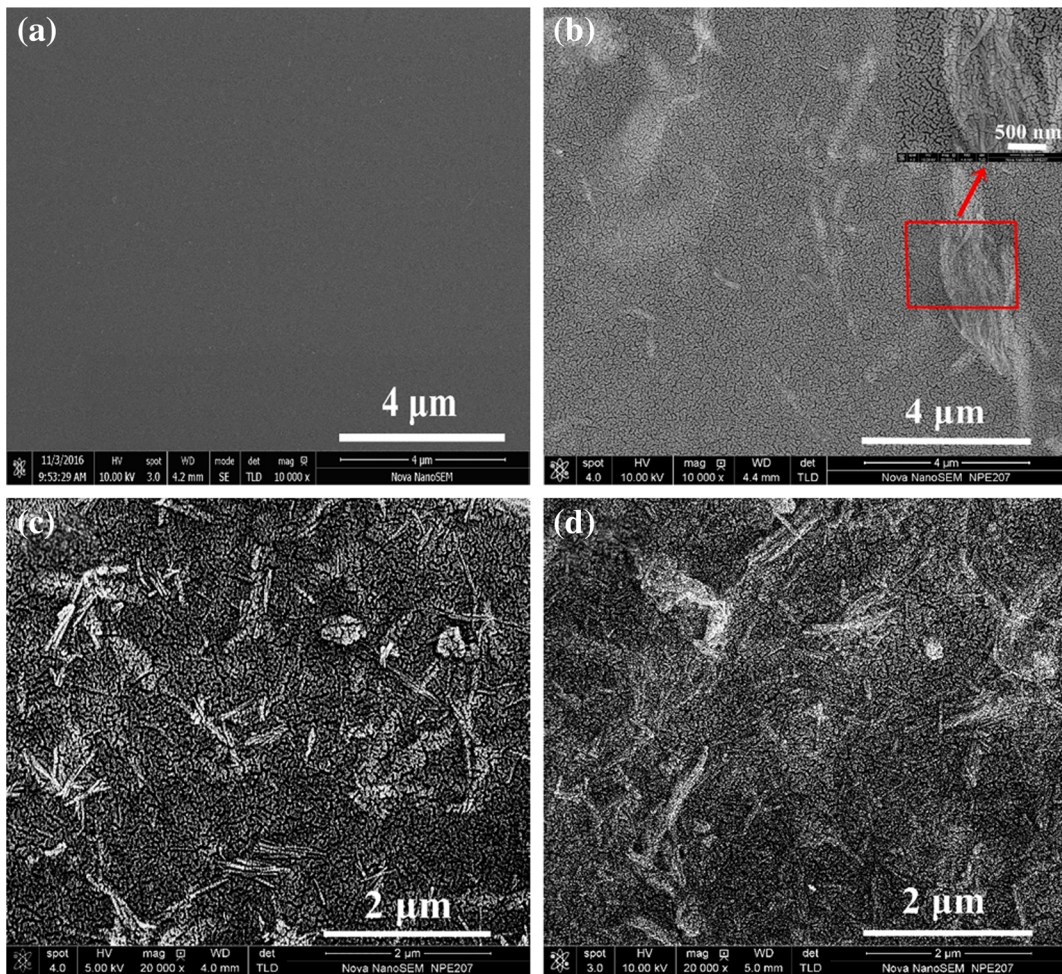
Fig. 3 Surface FESEM images of **a** the pristine PEDOT/PSS film and PEDOT/PSS/Te composite films with **b** 20, **c** 60, and **d** 85 wt.% Te nanorods

composite system. Whereas the PEDOT/PSS/Te composite films show a much higher electrical conductivity than either the pristine PEDOT/PSS or the Te nanorods. It is probably that a conformationally organized PEDOT/PSS interfacial layer (Fig. 2b, c) templated by the Te nanorods produces a higher conductivity in the polymer/nanocrystal composites than in the bulk PEDOT/PSS itself (See et al. 2010).

Although the PEDOT/PSS/Te composite films show high Seebeck coefficient, their electrical conductivity is still very low. To overcome this poor electrical conductivity, we treated the PEDOT/PSS/Te composite films with H_2SO_4. The room-temperature TE properties of the thin films treated with 9 M H_2SO_4 are shown in Fig. 5. The H_2SO_4 treatment has caused a marked increase in the electrical conductivity for all the composite films.
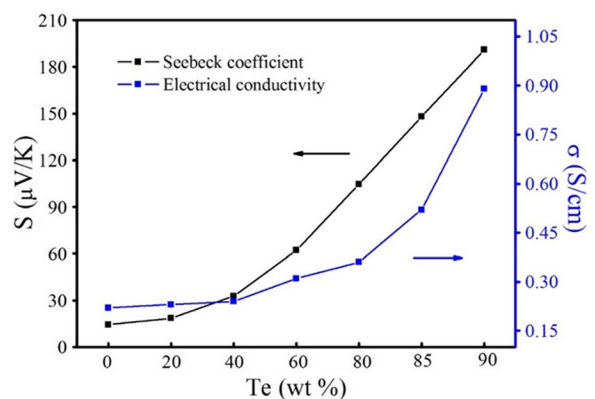
Fig. 4 Electrical conductivity σ, Seebeck coefficient S of PEDOT/PSS/Te-nanorod composite films as a function of Te content at room temperature
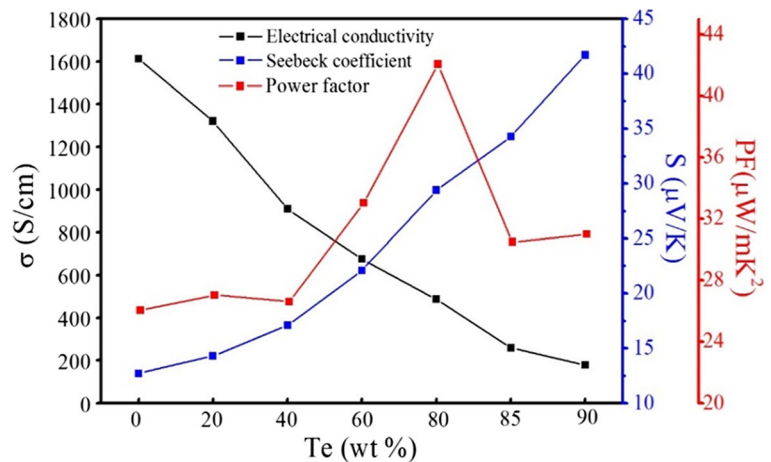
Especially for the pristine PEDOT/PSS, its electrical
conductivity increases sharply from 0.22 to 1613 S/
cm. Conversely, the Seebeck coefficient decreases after
the treatment. The Seebeck coefficient of the sample
containing 90 wt.% Te nanorods decreases from 191 to
41.7 μV/K. To clarify the effect of H_2SO_4 treatment,
morphology (see FESEM image in Fig. S1, Electronic
supplementary material) and TE transport parameters
(Tables S1 and S2, Electronic supplementary material)
of Te-nanorod film before and after the H_2SO_4 treatment
were characterized. After the H_2SO_4 treatment, the di-
ameter of the Te nanorods slightly increased and the
surface of the nanorods became rough due to the corro-
sion of the strong acid and elevated temperature during
the H_2SO_4 treatment. But the morphology of nanorods
is well maintained and the nanorods remained intercon-
nected with each other. Also, the H_2SO_4 treatment has
caused some changes in the TE properties of Te-nanorod
film: the electrical conductivity was slightly enhanced
(0.05 to 0.075 S/cm) along with a slight decrease in
Seebeck coefficient (370 to 345 μV/K), also the carrier
concentration is slightly enhanced. This is mainly attrib-
uted to the morphology and surface changes of the Te
nanorods after the H_2SO_4 treatment. On the whole, the
H_2SO_4 treatment indeed influenced the TE properties to
some extent. However, in consideration of that in the
PEDOT/PSS/Te-nanorod composite, the Te nanorods
are probably located at the bottom of the film due to
their higher density and coated with PEDOT/PSS, the
influence of the H_2SO_4 treatment is believed to be
mainly acted on PEDOT/PSS (carrier concentration of
PEDOT/PSS has been enhanced from 10^{19} cm^{-3} for the
pristine PEDOT/PSS to 10^{22} cm^{-3} after being treated
with H_2SO_4, Electronic supplementary material

Table S1) instead of Te nanorods. Despite the decrease
in Seebeck coefficient, the significantly enhanced elec-
trical conductivity results in a much higher PF compared
to that of the untreated PEDOT/PSS/Te composite films.
The highest PF of the H_2SO_4-treated PEDOT/PSS/Te
composite film is 42.1 μW/mK^2 obtained from the film
with 80 wt.% Te nanorods, which is more than 10 times
greater than that of the untreated PEDOT/PSS/Te com-
posite films and twice as great as that of the treated
PEDOT/PSS film. The power factor is higher than that
of the reported PEDOT/PSS/reduced graphene compos-
ite films (32.6 μW/mK^2) (Li et al. 2014) or PEDOT/
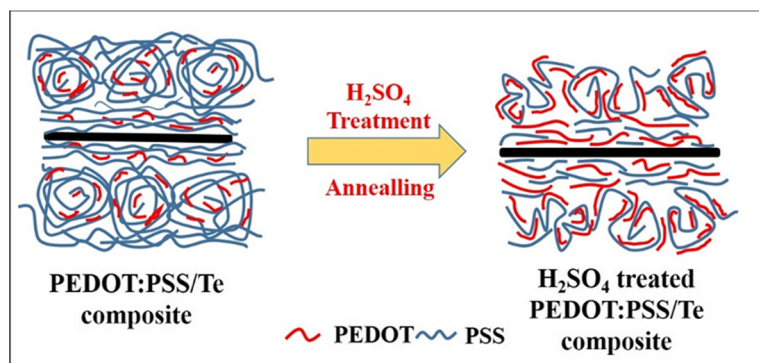PSS/Bi_2Te_3 based alloy nanosheet composite films
(32.26 μW/mK^2) (Kim et al. 2014).

The enhanced electrical conductivity of the H_2SO_4-
treated PEDOT/PSS/Te composite films is believed to
arise from the structural rearrangement of PEDOT/PSS.
XPS is used to analyze the surface chemical composi-
tion of the composite films to reveal the conformational
and compositional changes induced by the H_2SO_4 treat-
ment. Figure 6a presents the XPS survey spectra of the
pristine PEDOT/PSS and PEDOT/PSS/Te composite
films before (Fig. 6a (a, c)) and after the H_2SO_4 treat-
ment (Fig. 6a (b, d)). The H_2SO_4 treatment has not made
any obvious difference for the films in the survey spec-
tra. After forming composite with Te nanorods, strong
peaks at binding energy of 587 and 576 eV appear,
corresponding to the Te 3d3/2 and Te 3d5/2 peaks
(Mandale and Badrinarayanan 1990). Figure 6b shows
the characteristic peaks of S(2p) spectra of PEDOT/PSS
and PEDOT/PSS/Te before (Fig. 6b (a, c)) and after
(Fig. 6b (b, d)) treatment with H_2SO_4. Because the
sulfur atoms of the thiophene unit in PEDOT and of
the sulfonate group in PSS have different binding

(a)

(b)
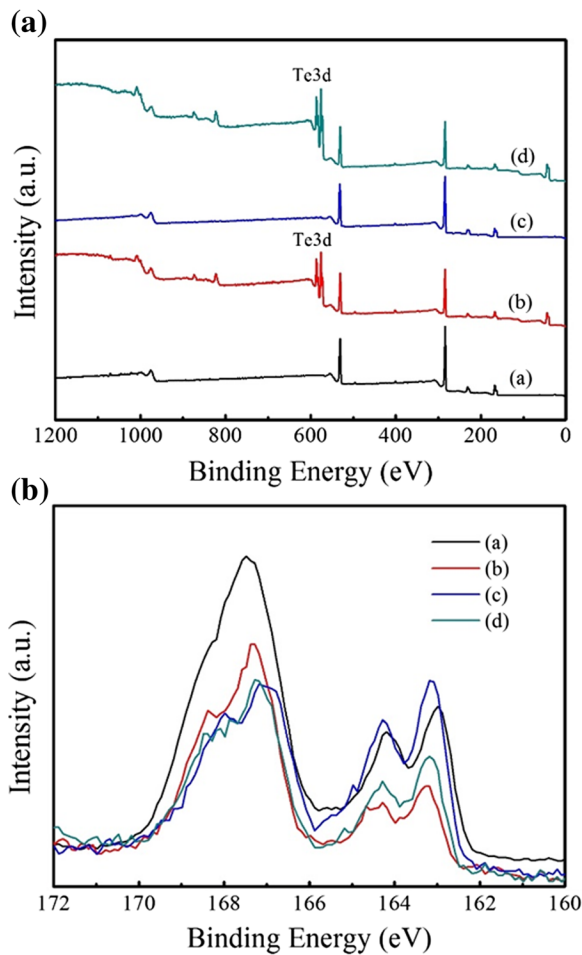
Fig. 6 XPS survey spectra (**a**) and sulfur S(2p) spectra (**b**) of the PEDOT/PSS film before (*a*) and after (*c*) the H$_2$SO$_4$ treatment; PEDOT/PSS/Te composite film with 60 wt.% Te nanorods before (*b*) and after (*d*) the H$_2$SO$_4$ treatment

energies, they exhibit two distinct types of sulfur atoms in the S2p peak characteristics. The broad peak at higher binding energy of 166–170 eV originates from the sulfur atoms in the PSS units, whereas the peak with a lower

binding energy of 162–166 eV corresponds to the sulfur atoms in the PEDOT units (Crispin et al. 2006).

Obviously, the H$_2$SO$_4$ treatment resulted in a reduction of the intensity of S(2p) from PSS and enhancement of the intensity of S(2p) from PEDOT (Fig. 6b (a–c, b–d)). The ratio of the S2p peak area of PSS to that of PEDOT can be used to estimate the relative composition of PSS to PEDOT at the film surface. This value is calculated by the ratio of the integral area of peaks assigned to PSS and PEDOT. The PSS/PEDOT ratios for pristine PEDOT/PSS and PEDOT/PSS/Te (60 wt.%) were 3.3 and 2.8 without H$_2$SO$_4$ treatment, and decrease to 1.6 and 1.8 for the H$_2$SO$_4$-treated films, respectively. The decrease of the PSS/PEDOT ratio indicates the removal of the insulating PSS from the film surface. The removal of PSS can induce a more crystalline structure of PEDOT, which is beneficial for the transport of carriers (Kim et al. 2014; Massonnet et al. 2015). The removal of PSS leads to easier intra- and inter-chain charge hopping.

A model is proposed to explain the mechanism of conductivity enhancement by the H$_2$SO$_4$ treatment as shown in Fig. 7. During the treatment, H$_2$SO$_4$ dissociates into H$^+$ and HSO$_4^-$ with pK_{a1} = −6.4. Since pK_{a1} of H$_2$SO$_4$ is higher than pK_a of PSSH (PSSH → PSS$^-$ + H$^+$, pK_a = −2.8), PSS$^-$ units get protonated upon treatment with sulphuric acid (H$^+$ + PSS$^-$ → PSSH). Therefore, the total reaction can be expressed as:

$$H_2SO_4 + PSS^- \rightarrow HSO_4^- + PSSH \tag{3}$$
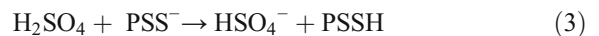
This results in the replacement of some PSS$^-$ with HSO$_4^-$ as the counter anions of PEDOT. Neutral PSSH units cannot exhibit Coulombic attractions with PEDOT grains, resulting in the phase segregation between the hydrophilic PSSH and hydrophobic PEDOT chains.

Fig. 7 Schematic illustration of the mechanism of conductivity enhancement of PEDOT/PSS films by the H$_2$SO$_4$ treatment

Besides, due to the coiled PSS$^-$ conformation and the Coulombic interactions between PSS$^-$ and positively charged PEDOT, PEDOT has a coil conformation in the pristine PEDOT/PSS (Xia and Ouyang 2011). The positive charges on the PEDOT chains are localized by the coil conformation, which hinders the transportation of the carriers. The H$_2$SO$_4$ treatment results in the disappearance of Coulombic attraction between PEDOT and PSSH; hence, the conformation of PEDOT changes from the coil to extended coil or linear structure, making the positive charges on PEDOT more delocalized.

Owing to the change in the structure of PEDOT/PSS caused by removing some of PSS upon the H$_2$SO$_4$ treatment, the values of carrier concentration has been dramatically enhanced from 10^{19} to 10^{22} cm^{-3}, while the Seebeck coefficient is inversely proportional to the n, $S \sim 1/n$ (Snyder and Toberer 2008). Therefore, the decrease in the Seebeck coefficient after being treated with H$_2$SO$_4$ is due to an increase in the n value of the composites.

For the inorganic TE materials, thermal conductivity increases with electrical conductivity due to the Wiedemann-Franz law. However, organic conducting polymers do not obey the Wiedemann-Franz law, and there is weak correlation between electrical conductivity and thermal conductivity. The thermal conductivity of conducting polymers is intrinsically low, which provides them a great potential probability of TE application compared with inorganic materials. Typically, the thermal conductivity of PEDOT/PSS is around 0.2 W/mK (Kim et al. 2013; See et al. 2010; Jiang et al. 2008), which is about one order of magnitude lower than that of the Te (2 W/mK, bulk value (See et al. 2010)). Previous studies have shown that the polymer matrix dominates the total thermal conductivity in polymer/inorganic composite system, such as in situ-synthesized PEDOT/PSS/Te-nanorod composite with a thermal conductivity of about 0.22–0.3 W/mK (86.47 wt.% Te, See et al. 2010) and PANI/Te (70 wt.%) nanocomposite with a thermal conductivity of ~0.2 W/mK (Wang et al. 2016). In this work, the Te nanorods are imbedded in the PEDOT/PSS matrix and the rod-rod junctions are connected by the PEDOT/PSS, combined with the phonon scattering effect results from the Te-nanorod/PEDOT/PSS interfaces (Coates et al. 2013), the thermal conductivity of the composite films is believed to be similar to or even lower than that of the pure PEDOT/PSS. If the thermal conductivity of 0.2 W/mK is taken to calculate the ZT value of the composite films, the ZT value is around 0.063 at room temperature for the H$_2$SO$_4$-treated composite film containing 80 wt.% Te nanorods.

Conclusions

Two strategies have been used to enhance the TE properties of PEDOT/PSS. Through added Te nanorods, the Seebeck coefficient has increased to 191 µV/K (90 wt.% Te) due to the high Seebeck coefficient of the Te nanorods. The H$_2$SO$_4$ treatment has then used to further improve the TE properties of the PEDOT/PSS/Te composite films through adjusting the doping levels and increasing the carrier concentrations. XPS analyses show the removal of insulating PSS in the PEDOT/PSS during the H$_2$SO$_4$ treatment, resulting in a structural rearrangement of PEDOT/PSS and increased carrier concentrations. The electrical conductivity has drastically enhanced from 0.22 to 1613 S/cm. Despite the decline in the Seebeck coefficient of the PEDOT/PSS/Te composite films, an optimum power factor of 42.1 µW/mK^2 has been obtained at room temperature from a PEDOT/PSS/Te composite film containing 80 wt.% Te nanorods, which is about ten times greater than that of the untreated PEDOT/PSS/Te composite film. This work provides a simple approach to design and adjust the TE properties of conducting polymer/inorganic nanostructure composites.

Compliance with ethical standards

Conflict of interest The authors declare that they have no conflict of interest.

References

Bubnova O, Khan ZU, Malti A, Braun S, Fahlman M, Berggren M, Crispin X (2011) Optimization of the thermoelectric figure of merit in the conducting polymer poly (3,4-ethylenedioxythiophene). Nat Mater 10:429–433

Cao YQ, Zhao XB, Zhu TJ, Zhang XB, JP T (2008) Syntheses and thermoelectric properties of Bi2Te3/Sb2Te3 bulk nanocomposites with laminated nanostructure. Appl Phys Lett 92: 143106

Choi J, Lee J Y, Lee S-S, Park CR, Kim H (2016) High-performance thermoelectric paper based on double carrier-filtering processes at nanowire heterojunctions. Adv Energy Mater 1502181

Coates NE, Yee SK, McCulloch B, See KC, Majumdar A, Segalman RA, Urban JJ (2013) Effect of interfacial properties on polymer–nanocrystal thermoelectric transport. Adv Mater 25:1629–1633

Crispin X, Jakobsson FLE, Crispin A, Grim PCM, Andersson P, Volodin A, van Haesendonck C, Van der Auweraer M, Salaneck WR, Berggren M (2006) The origin of the high conductivity of poly(3,4-ethylenedioxythiophene)-poly (styrenesulfonate) (PEDOT-PSS) plastic electrodes. Chem Mater 18:4354–4360

Du Y, Cai KF, Chen S, Cizek P, Lin T (2014) Facile preparation and thermoelectric properties of Bi2Te3 based alloy nanosheet/PEDOT:PSS composite films. ACS Appl Mater Interfaces 6:5735–5743

Du Y, Shen SZ, Cai KF, Casey PS (2012) Research progress on polymer–inorganic thermoelectric nanocomposite materials. Prog Polym Sci 37:820–841

Dun C, Hewitt CA, Huang H, Montgomery DS, Xu J, Carroll DL (2015) Flexible thermoelectric fabrics based on self-assembled tellurium nanorods with a large power factor. Phys Chem Chem Phys 17:8591–8595

Han Z, Alberto F (2011) Thermal conductivity of carbon nanotubes and their polymer nanocomposites: a review. Prog Polym Sci 36:914–940

He M, Qiu F, Lin ZQ (2013) Towards high-performance polymer-based thermoelectric materials. Energy Environ Sci 6:1352–1361

Jiang FX, JK X, BY L, Xie Y, Huang RJ, Li LF (2008) Thermoelectric performance of poly (3, 4-ethylenedioxythiophene):poly (styrenesulfonate). Chin Phys Lett 25:2202–2205

Ju H, Kim J (2016) Chemically exfoliated SnSe Nanosheets and their SnSe/poly(3,4-ethylenedioxythiophene): poly(styrenesulfonate) composite films for polymer based thermoelectric applications. ACS Nano 10:5730–5739

Kim D, Kim Y, Choi K, Grunlan JC, Yu C (2009) Improved thermoelectric behavior of nanotube-filled polymer composites with poly(3,4-ethylenedioxythiophene) poly(styrenesulfonate). ACS Nano 4:513–523

Kim G-H, Shao L, Zhang K, Pipe KP (2013) Engineered doping of organic semiconductors for enhanced thermoelectric efficiency. Nat Mater 12:719–723

Kim N, Kee S, Lee SH, Lee BH, Kahng YH, Jo Y-R, Kim B-J, Lee K (2014) Highly conductive PEDOT:PSS nanofibrils induced by solution-processed crystallization. Adv Mater 26: 2268–2272

Li FY, Cai KF, Shen SZ, Chen S (2014) Preparation and thermoelectric properties of reduced graphene oxide/PEDOT: PSS composite films. Synth Met 197:58–61

Mandale AB, Badrinarayanan S (1990) X-ray photoelectron spectroscopic studies of the semimagnetic semiconductor system $Pb_{1-x}Mn_xTe$. J Electron Spectrosc Relat Phemon 53:87–95

Massonnet N, Carella A, de Geyer A, Faure-Vincent J, Simonato J-P (2015) Metallic behaviour of acid doped highly conductive polymers. Chem Sci 6:412–417

Murphy CJ, Jana NR (2002) Controlling the aspect ratio of inorganic nanorods and nanowires. Adv Mater 14:80–82

Pal S, Balasubramanian G, Puri IK (2013) Reducing thermal transport in electrically conducting polymers: effects of ordered mixing of polymer chains. Appl Phys Lett 102:023109

Pang H, Piao YY, Tan YQ, Jiang GY, Wang JH, Li ZM (2013) Thermoelectric behaviour of segregated conductive polymer composites with hybrid fillers of carbon nanotube and bismuth telluride. Mater Lett 107:150–153

See KC, Feser JP, Chen CE, Majumdar A, Urban JJ, Segalman RA (2010) Water-processable polymer–nanocrystal hybrids for thermoelectrics. Nano Lett 10:4664–4667

Snyder GJ, Toberer ES (2008) Complex thermoelectric materials. Nat Mater 7(105):114

Song HJ, Cai KF, Wang J, Shen S (2016) Influence of polymerization method on the thermoelectric properties of multi-walled carbon nanotubes/polypyrrole composites. Synth Met 211:58–65

Venkatasubramanian R, Siivola E, Colpitts T, O'Quinn B (2001) Thin-film thermoelectric devices with high room-temperature figures of merit. Nature 413:597–602

Wang H, Hsu J-H, Yi S-I, Kim S, Choi K, Wang G, Yu C (2015a) Thermally driven large N-type voltage responses from hybrids of carbon nanotubes and poly(3,4-ethylenedioxythiophene) with tetrakis(dimethylamino) ethylene. Adv Mater 27:6855–6861

Wang J, Cai KF, Shen S (2015b) A facile chemical reduction approach for effectively tuning thermoelectric properties of PEDOT films. Org Electron 17:151–158

Wang J, Cai KF, Shen S, Yin JL (2014) Preparation and thermoelectric properties of multi-walled carbon nanotubes/polypyrrole composites. Synth Met 195:132–136

Wang Y, Zhang SM, Deng Y (2016) Flexible low-grade energy utilization devices based on high-performance thermoelectric polyaniline/tellurium nanorod hybrid films. J Mater Chem A 4:3554–3559

Wang YJ (2009) Research progress on a novel conductive polymer–poly(3,4-ethylenedioxythiophene) (PEDOT). J Phys Conf Ser 152

Weathers A, Khan ZU, Brooke R, Evans D, Pettes MT, Andreasen JW, Crispin X, Shi L (2015) Significant electronic thermal transport in the conducting polymer poly(3,4-ethylenedioxythiophene). Adv Mater 27:2101–2106

Xi G, Liu Y, Wang X, Liu X, Peng Y, Qian Y (2006) Large-scale synthesis, growth mechanism, and photoluminescence of ultrathin Te nanowires. Cryst Growth Des 6:2567–2570

Xia Y, Ouyang J (2011) PEDOT:PSS films with significantly enhanced conductivities induced by preferential solvation with cosolvents and their application in polymer photovoltaic cells. J Mater Chem 21:4927–4936

Xiong J, Jiang F, Shi H, Xu J, Liu C, Zhou W, Jiang Q, Zhu Z, Hu Y (2015) Liquid exfoliated graphene as dopant for improving the thermoelectric power factor of conductive PEDOT:PSS nanofilm with hydrazine treatment. ACS Appl Mater Interfaces 7:14917–14925

Yu C, Choi K, Yin L, Grunlan JC (2011) Light-weight flexible carbon nanotube based organic composites with large thermoelectric power factors. ACS Nano 5:7885–7892